Ultrasonics Sonochemistry 112 (2025) 107215

Contents lists available at ScienceDirect

Ultrasonics Sonochemistry

journal homepage: www.elsevier.com/locate/ultson

Mild ultrasound-assisted alkali de-esterification modified pectins: Characterization and structure–activity relationships in immunomodulatory effects

Huan Guo [a], Dong Li [a,b], Baohe Miao [c,*], Kanglin Feng [d], Guijing Chen [e], Renyou Gan [f], Zhiliang Kang [g], Hong Gao [a,*]

[a] College of Biomass Science and Engineering and Healthy Food Evaluation Research Center, Sichuan University, Chengdu 610065, China
[b] Department of Food Science and Engineering, Moutai Institute, Renhuai 564502, China
[c] Institute of Urban Agriculture, Chinese Academy of Agricultural Sciences, National Agricultural Science and Technology Center, Chengdu 610213, China
[d] Fruit and Vegetable Storage and Processing Research Center, Institute of Agricultural Products Processing, Sichuan Academy of Agricultural Sciences, Chengdu 610066, China
[e] Sichuan University-The Hong Kong Polytechnic University Institute for Disaster Management and Reconstruction, Chengdu 610200, China
[f] Department of Food Science and Nutrition, Faculty of Science, The Hong Kong Polytechnic University, Kowloon, Hong Kong
[g] College of Mechanical and Electrical Engineering, Sichuan Agricultural University, Ya'an, Sichuan 625014, China

ARTICLE INFO

Keywords:
Apple pectin
Esterification degree
Gut microbiota
Immunomodulatory activity
Structure-activity relationship

ABSTRACT

Apple pectin (AP), a well-established dietary fiber, offers significant health benefits, particularly in immunomodulation. However, the structure–activity relationship (SAR) in this context remains poorly understood. This study aimed to elucidate the impact of varying degrees of esterification (DE) on AP's SAR in immunomodulatory activity. AP-Es (AP-E1, AP-E2, AP-E3) with different DE were prepared using mild ultrasound-assisted alkali de-esterification, followed by SAR analysis. Results revealed that AP-E3, with the lowest DE (5.08 ± 0.22 %), demonstrated a significant reduction in homogalacturonan (HG) domains and a corresponding increase in rhamnogalacturonan-I (RG-I) domains, which coincided with enhanced immunomodulatory effects. The molecular weights of AP-E1, AP-E2, and AP-E3 were determined to be 30.94 ± 0.83 kDa, 27.61 ± 0.65 kDa, and 22.17 ± 0.57 kDa, respectively. To further explore the underlying mechanism, transgenic zebrafish with fluorescent macrophages were utilized. A positive correlation was observed between AP-E3 concentration and the number of fluorescent microspheres engulfed by macrophages. Additionally, AP-E3 significantly upregulated the expression of key immune response genes (*tnf-α*, *il-1β*, *il-6*, *cox-2*, *inos*, and *nf-κb*) and restored the gut microbiota composition and abundance in chloramphenicol-induced immunocompromised zebrafish. Metabolomics analysis revealed that AP-E3 effectively restored metabolic homeostasis by activating multiple signaling pathways associated with signal transduction, immune regulation, and metabolism. These findings highlight the potential of low-esterified AP enriched with RG-I domains as a promising candidate for applications in immune modulation and gut health management.

1. Introduction

The apple industry holds a significant position in global agriculture, with China being the largest producer of apples worldwide. Apples are not only an important economic crop but also widely appreciated for their rich nutritional content and various bioactive components, including dietary fiber (particularly pectin), polyphenols, organic acids, vitamins, and minerals [1]. Pectin, a vital dietary fiber abundantly found in apples, is primarily located in the peel and pulp. It can be classified into three major types based on its structure: homogalacturonan (HG), rhamnogalacturonan-I (RG-I), and rhamnogalacturonan-II (RG-II) [2]. Furthermore, pectin can be categorized based on its degree of esterification (DE) into high-esterified pectin (DE > 50 %) and low-esterified pectin (DE < 50 %) [3]. Pectin possesses diverse biological properties that contribute significantly to human health such as anti-cancer, gut microbiota modulation, and immunomodulatory effects. Numerous

* Corresponding authors.
E-mail addresses: miaobaohe@163.com (B. Miao), gh@scu.edu.cn (H. Gao).

https://doi.org/10.1016/j.ultsonch.2024.107215
Received 7 November 2024; Received in revised form 24 December 2024; Accepted 28 December 2024
Available online 30 December 2024

studies have demonstrated the ability of pectin to modulate gut composition and function, thereby promoting gut health. For instance, supplementation with apple-derived pectin has been shown to increase levels of beneficial gut bacteria such as *Akkermansia* and *Lachnospiraceae* UCG-010, which are associated with improved gut health and reduced inflammation [4]. Moreover, pectin exhibits significant immunomodulatory effects by enhancing the body's immune response. In our previous study, AP has been found to stimulate the production of cytokines such as IL-6 and TNF-α, which play crucial roles in immune regulation [5].

Previous studies have reported that appropriate ultrasound-assisted/alkali treatment can effectively reduce the esterification degree of high-esterified pectin, leading to a decrease in its HG domains and an increase in RG-I domains [6–8]. Moreover, ultrasound/alkali-treated pectin exhibits a shorter and smaller molecular structure with reduced entanglement [6,8]. Low-esterified pectin typically possesses superior biological properties compared to other types of pectin. For example, Fan et al. [9] reported that low-esterified pectin demonstrated protective effects in acute colitis mice. Furthermore, studies have indicated that pectin with a lower degree of esterification can enhance immunoactivity. For example, Li et al. [10] found that mild alkali de-esterification improved the immunostimulatory activity of pectin from *Fagopyrum tataricum* (L.) Gaertn leaves. Additionally, alkali treatment was shown to yield quinoa microgreens' pectic polysaccharides with a lower degree of esterification, which enhanced their immunostimulatory activity by activating the TLR4/NF-κB signaling pathway [11]. Despite existing reports on the immunostimulatory activity of de-esterified pectin polysaccharides, there is still a lack of *in vivo* studies investigating this phenomenon comprehensively. Moreover, the precise mechanisms through which structural features like the degree of esterification and RG-I domains influence gut microbiota and immunomodulation remain incompletely understood. We hypothesized that the immunostimulatory activity of apple pectin was enhanced by increasing the RG-I domain of the pectin.

Zebrafish *(Danio rerio)* has rapidly emerged as a well-recognized animal model for investigating host-microbe-immune interactions, owing to their genetic similarity to humans, transparent embryos, cheap housing costs, genetic tractability, and rapid developmental cycles [12,13]. In particular, the advent of transgenic zebrafish models with fluorescently labeled macrophages has revolutionized the exploration of immune regulation and host-microbe interactions. These transgenic models enable real-time *in vivo* visualization of macrophage behavior and function, thereby providing novel insights into the innate immune responses and their modulation by gut microbiota [14].

Therefore, to elucidate the SAR of AP, a mild ultrasound-assisted alkali de-esterification method was employed for precise modification of AP. This study systematically investigated the effects of various esterification degrees on the immunomodulatory properties of AP. Furthermore, we conducted 16S rRNA sequencing and metabolomics analysis in zebrafish to explore the immunomodulatory mechanisms of low esterification pectin. These findings contribute to a comprehensive understanding of the precise SAR of AP and promote its applications in the food industry.

2. Materials and methods

2.1. Materials and chemicals

The apples (*Malus pumila* Mill.) were harvested in mid-September from Hanyuan County, Ya'an City, China. Lipopolysaccharide (LPS), standard monosaccharides, and MTT Cell Proliferation and Cytotoxicity Assay Kit were purchased from Sigma-Aldrich (MA, USA). RAW 264.7 cells were obtained from the Cell Bank of the Chinese Academy of Sciences (Shanghai, China). Wild-type zebrafish (AB strain) and transgenic zebrafish with fluorescent macrophages were provided by the Yishulihua Biotechnology Co. (Nanjing, China). Chloramphenicol and berberine hydrochloride were purchased from RHAWN reagent (Shanghai, China). Additionally, all the other chemicals and reagents used in this study were of analytical grade.

2.2. Extraction and purification of native AP

The extraction and purification of AP were performed according to our previously established protocol [5]. Briefly, 100 g of apple pomace powder was refluxed with 1000 mL of 80 % (*v/v*) ethanol in an ultrasonic bath at 40 °C for 30 min. Subsequently, the crude apple pectin was extracted twice with 2000 mL of ultrapure water in a boiling water bath for 2 h. The resulting precipitate was washed twice with 70 % ethanol, redissolved in pure water at 80 °C, and transferred to dialysis membranes (molecular weight cutoff: 3.5 kDa) for dialysis over 4 d. Finally, the obtained solution was freeze-dried at − 40 °C for 48 h to obtain crude apple pectin from the apple pomace powder. Subsequently, crude AP (10 mg/mL) was loaded onto a DEAE-cellulose column (Ø 4.5 × 60 cm). Sequential elution from the column was carried out using ultrapure water, followed by NaCl solutions, gradually increasing in concentrations from 0.1 M to 0.5 M, at an elution rate of 3 mL/min. The fraction eluted with 0.1 M NaCl underwent further purification using a Sephacryl S-300 HR column (Ø 2.5 × 60 cm), employing a mobile phase consisting of 0.1 M NaCl as the eluent. Finally, the eluate was dialyzed and freeze-dried to obtain purified native AP (AP-E1).

2.3. Preparation of AP with different degrees of esterification

The mild ultrasound-assisted alkali de-esterification method was adapted from the reported procedure with slight modifications [8,11]. Briefly, native AP (AP-E1, 5.0 mg/mL) was dissolved in NaOH solutions at pH 10.0 (0.1 mM), and then incubated by an ultrasonic cleaner (AS3120B, Beijing HengAoDe Instrumentation Co., 40 kHz) at 25 °C for 30 min and 60 min, respectively. Subsequently, the pH of the reaction mixture was adjusted to pH 6.0 using hydrochloric acid, and precipitation occurred upon the addition of three times the volume of 95 % ethanol (*v/v*). The resulting precipitate underwent dissolution while removing small molecules through dialysis bags (>3 kDa). Finally, AP-E2 and AP-E3 were obtained as modified pectin samples representing medium and low degrees of esterification, respectively; these samples were stored at 4 °C until further analysis.

2.4. Determination of the chemical composition of AP-Es

The total polysaccharide content of AP-Es was determined using the phenol–sulfuric acid method [15]. Uronic acids and proteins in AP-Es were quantified by the m-hydroxydiphenyl method [16] and Bradford's method [17], respectively. Additionally, a PerkinElmer Lambda 1050 UV/Vis spectrophotometer (Perkin Elmer Corp., Massachusetts, USA) was utilized to obtain the UV spectrum of an AP-Es solution (1.0 mg/mL) for assessing the presence of nucleic acids and proteins.

2.5. Determination of structural properties of AP-Es

2.5.1. Determination of homogeneity and molecular weight

The molecular weight (M_w), homogeneity, and chain conformational parameters of AP-Es were evaluated using size exclusion chromatography combined with multi-angle laser light scattering and refractive index detectors (SEC-MALLS-RI) system on a U3000 HPLC apparatus (Thermo Fisher Scientific, Waltham, MA, USA). The experimental procedures followed the protocol described in a previous study [18].

2.5.2. Monosaccharide composition

The monosaccharide compositions of the AP-Es were analyzed using high-performance anion-exchange chromatography (HPAEC) on a Thermo ICS 5000 + chromatographic system (Thermo Fisher Scientific, Wal tham, MA, USA), equipped with a Dionex™ CarboPac™ PA-20 anion- exchange column (3 × 150 mm, 10 μm) and a pulsed

amperometric detector (PAD). The hydrolysis procedure followed a previously described method [19]. The HPAEC analysis was conducted with the following optimized parameters: column temperature maintained at 30°C, injection volume set to 5 μL, and flow rate adjusted at 0.5 mL/min.

2.5.3. Fourier transform infrared (FT-IR) spectroscopy

The FT-IR spectra analysis of three AP-Es was performed in the range of 400 − 4000 cm^{-1} using a Nicolet iS10 Fourier transform infrared spectroscopy instrument (ThermoFisher Scientific, Waltham, MA, USA). The DE values were calculated following the methodology reported by Chatjigakis et al. [20].

2.6. Determination of the immunomodulatory activity of AP-Es in vitro

The immunomodulatory effects of AP-Es with different degrees of esterification on RAW 264.7 cells were determined according to our previously described method [5] to identify the optimal apple pectin for immunomodulatory.

2.7. Determination of the immunomodulatory activity of AP-E3 in vivo

2.7.1. Determination of the effect of AP-E3 on zebrafish macrophages

The effect of AP-Es on macrophages was assessed using transgenic zebrafish with fluorescently labeled macrophages. Zebrafish were reared according to the previously described method (Fig. 3A) [21]. All zebrafish were maintained under controlled conditions (28 ± 0.5 °C, 14/10 h light/dark cycle). No additional food was provided until the yolk sac was consumed (4 dpf). At 5 dpf, zebrafish were randomly divided into six groups: blank control (Con), model (MC), positive control (PC), AP-E3/L (250 μg/mL), AP-E3/M (500 μg/mL), and AP-E3/H (1000 μg/mL). Chloramphenicol (150 μg/mL) and berberine hydrochloride (5.33 μg/mL) were used to induce immunocompromised models and serve as positive controls, respectively. Zebrafish tolerance was evaluated by monitoring the mortality rate of 100 zebrafish juveniles after 24 h. The number of fluorescently labeled macrophages in zebrafish was visualized by a stereoscopic microscope (SZX7, OLYMPUS, Tokyo, Japan).

2.7.2. Measurement of the NO production in zebrafish

The Zebrafish were reared according to the procedure described in Section 2.6.1. Paramecia were provided as feed from 5 to 8 days post-fertilization (dpf), while boiled egg yolk was filtered through a 20 μm mesh from 9 to 11 dpf. On the 12th dpf, Zebrafish samples were collected to assess nitric oxide (NO) production. The production of NO was quantified using previously described kits following the method [22].

2.7.3. Determination of the mRNA expression of inos, cox-2, il-6, il-1β, nf-κb, and tnf-α in zebrafish

The relative mRNA expression of *inos, cox-2, il-6, il-1β, nf-κb,* and *tnf-α* in zebrafish (12th dpf) was assessed using a CFX Connect Real-Time Quantitative Polymerase Chain Reaction system (Bio-Rad, Hercules, CA, USA), as described in our previous method [22]. Primer sequences for amplification are provided in Table S1.

2.7.4. Gut microbiota analysis of zebrafish

The PF Mag-Bind Stool DNA Kit (Omega Bio-tek, Georgia, U.S.) was employed for the extraction of total microbial genomic DNA from zebrafish. The quality and concentration of the DNA were assessed with a NanoDrop® ND-2000 spectrophotometer (Thermo Scientific Inc., USA) and 1.0 % agarose gel electrophoresis. Amplification of the V3-V4 hypervariable regions of the bacterial 16S rRNA gene was performed with primers 338F and 806R on an ABI GeneAmp® 9700 PCR thermocycler (ABI, CA, USA). The PCR cycling conditions followed the protocol [23]. Each sample was amplified in triplicate. PCR products were extracted from 2 % agarose gel, purified, and quantified using a Quantus™ Fluorometer (Promega, USA). The 16S rRNA gene amplicons were sequenced on the Illumina MiSeq platform at Shanghai Majorbio Biopharm Technology Co., Ltd. (Shanghai, China) as previously described [23]. Rarefaction curves and alpha diversity indices were calculated based on ASVs information using Mothur v1.30.2. Microbial community similarities among samples were assessed through Bray-Curtis Difference-based Principal Coordinate Analysis (PCoA) utilizing the Vegan v2.4.3 package.

2.7.5. Metagenome analysis of zebrafish

A 50 mg of zebrafish sample was collected in a 2 mL centrifuge tube for metabolite extraction, which was performed using 400 μL of an extraction solution (methanol: water = 4:1 (*v/v*)) containing 0.02 mg/mL of internal standard (L-2-chlorophenylalanine). LC-MS analysis was conducted on the UHPLC-Q Exactive system from Thermo Fisher Scientific. The mobile phases were 0.1 % formic acid in water (95:5, *v/v*) (solvent A) and 0.1 % formic acid in acetonitrile: isopropanol (47.5:47.5:5, *v/v*) (solvent B). The gradient conditions were: 0–0.1 min, 0 %–5% B, 0.1–2 min, 5 %–25 % B, 2–9 min, 25 %–100 % B, 9–13 min, 100 % B, 13–13.1 min, 100 %–0% B, 13.1–16 min, 0 % B. The sample injection volume was 2 μL with a flow rate of 0.4 mL/min, and the column temperature was maintained at 40 °C. The R package ropls (Version 1.6.2) was used to conduct principal component analysis (PCA) and orthogonal partial least squares discriminant analysis (OPLS-DA), employing 7-cycle interactive validation to assess model stability. Differential metabolites between the two groups were identified and their biochemical pathways were determined by conducting metabolic enrichment and pathway analysis using the KEGG database.

2.7.6. Ethical statement

The experimental animal protocols were approved by the Ethics Committee of West China Hospital, Sichuan University (approval no. Gwll2023132), and adhered to the guidelines set forth in the EU Directive 2010/63/EU for conducting animal experiments.

2.8. Statistical analysis

The experiments were performed in triplicate, and the data are presented as means ± standard deviation. Data analysis was performed using IBM SPSS Statistics 26 software (IBM, New York, USA). Differences among samples were analyzed by one-way analysis of variance (ANOVA) followed by post *hoc* Duncan's *test*. Additionally, Origin 2018 software (OriginLab Inc., Northampton, MA, USA) was utilized for charts plotting. Statistical significance was defined at $p < 0.05$.

3. Results and discussion

3.1. Physicochemical characteristics of AP-Es

3.1.1. Chemical composition

Crude pectin typically contains substantial amounts of phenolic acids, protein, and other impurities that can significantly influence their biological activities. Therefore, we quantitatively analyzed the phenolic acid and protein content in AP-Es. As shown in Table 1, no phenolic acid or protein was detected in AP-Es. In addition, the absence of peaks in the UV spectra at 260 nm and 280 nm (Fig. 1C) confirmed the above findings, indicating that the samples were free of impurities such as proteins, phenolic acids, and nucleic acids. Moreover, the total polysaccharides content of AP-Es ranged from 91.94 % to 93.22 %, with no significant differences.

3.1.2. Homogeneity and M_w

The SEC-MALLS-RI analysis not only provided M_w values but also demonstrated the homogeneity of the analyzed pectin. As depicted in Fig. 1A, the SEC-MALLS-RI chromatograms of AP-E1, AP-E2, and AP-E3

Table 1
Chemical analysis, M_w, and monosaccharide composition of AP-Es.

	AP-E1	AP-E2	AP-E3
Total polysaccharides (%)	91.94 ± 0.84 [a]	92.45 ± 0.67 [a]	93.22 ± 0.49[b]
Protein contents (%)	N.D.	N.D.	N.D.
Phenolic acids content (%)	N.D.	N.D.	N.D.
DE using FT-IR method (%)	55.17 ± 1.85 [a]	36.36 ± 1.43[b]	5.08 ± 0.22[c]
M_w ($\times 10^3$ Da)	30.94 ± 0.83 [a]	27.61 ± 0.65[b]	22.17 ± 0.57[c]
M_n ($\times 10^3$ Da)	24.15 ± 0.49 [a]	21.98 ± 0.46[b]	17.024 ± 0.42[c]
M_w/M_n	1.28	1.26	1.30
R_g	19.0 ± 0.24[c]	20.4 ± 0.18[b]	22.8 ± 0.25 [a]
$\alpha_s (R_g = kM_w^{\alpha_s})$	0.39	0.25	0.08
Monosaccharides and molar mass ratios			
Rha (%)	3.34	5.34	8.21
Ara (%)	7.37	12.07	33.8
Gal (%)	10.45	14.22	14.87
Glc (%)	1.64	3.04	6.19
GalA (%)	77.20	65.32	36.93
Rha/GalA	0.04	0.08	0.22
(Ara + Gal)/Rha	5.34	4.92	5.93
GalA/(Rha + Ara + Gal)	3.64	2.07	0.59
%HG (GalA-Rha)	73.86	59.98	28.72
%RG-I (2Rha + Ara + Gal)	24.50	36.97	65.09
HG/RG-I	3.01	1.62	0.44

Values represent mean ± standard deviation and statistical analysis was carried out by ANOVA plus *post hoc* Ducan's test, and statistical significance ($p < 0.05$) was indicated with different letters (a-c). Abbreviations: *Rg*, Radius of gyration; DE, degree of esterification; N.D., Not determined; Rha, Rhamnose; Ara, Arabinose; Gal, Galactose; Glc, Glucose; GalA, Galacturonic acid.

exhibited a rightward shift, indicating that mild ultrasound-assisted alkali treatment resulted in AP with lower molecular weight. Specifically, the M_w values of AP-E2 and AP-E3 were 27.61 × 10^3 and 22.17 × 10^3 Da, respectively (Table 1), which were significantly lower than that of AP-E1 (30.94 × 10^3 Da). Moreover, the polydispersity indices (M_w/M_n) of AP ranged from 1.26 to 1.30, consistent with the SEC-MALLS-RI chromatograms obtained. After mild ultrasound-assisted alkali treatment, there was a slight increase in the radius of gyration (R_g) of AP-Es (Fig. 1B). The R_g values estimated for AP-E1, AP-E2, and AP-E3 were found to be 19.0 nm, 20.4 nm, and 22.8 nm, respectively, revealing distinctive molecular characteristics of the pectin. Additionally, accumulating studies have demonstrated the impact of mild ultrasound-assisted alkali treatment and alkali treatment on the chain conformation of natural polysaccharides [6,8]. The conformational parameter α_s is closely associated with macromolecule shape [24]. Theoretically, α_s values of 0.33, 0.5–0.6, 0.6–1.0, and 1.0 correspond to conformations such as spheres, flexible chains, semi-flexible chains, and rigid rods, respectively [25]. As shown in Table 1, the determined α_s value for AP-E1 was found to be 0.39, indicating that its conformation resembled that of a sphere due to its low molecular weight. Moreover, it was observed that increasing ultrasound-assisted treatment time led to a gradual decrease in α_s values, suggesting enhanced coiling and bending of AP chains in aqueous solution resulting in more flexible conformations. Changes in M_w have been reported to influence chain conformation transitions; for example, β-D-glucan exhibited looser and more flexible chain conformations as its molecular weight decreased due to degradation through ultrasound-assisted H_2O_2/ascorbic acid reaction [26,27].

3.1.3. FT-IR spectrum analysis

The FT-IR spectra of AP-Es are presented in Fig. 1D, revealing characteristic signals associated with pectin-type polysaccharides, including peaks at 3433 cm^{-1}, 2926 cm^{-1}, 1745 cm^{-1}, 1617 cm^{-1}, 1420 cm^{-1}, 1101 cm^{-1}, and 1017 cm^{-1}. Generally, the peaks at 3433 cm^{-1} and 2926 cm^{-1} were attributed to hydroxyl group stretching

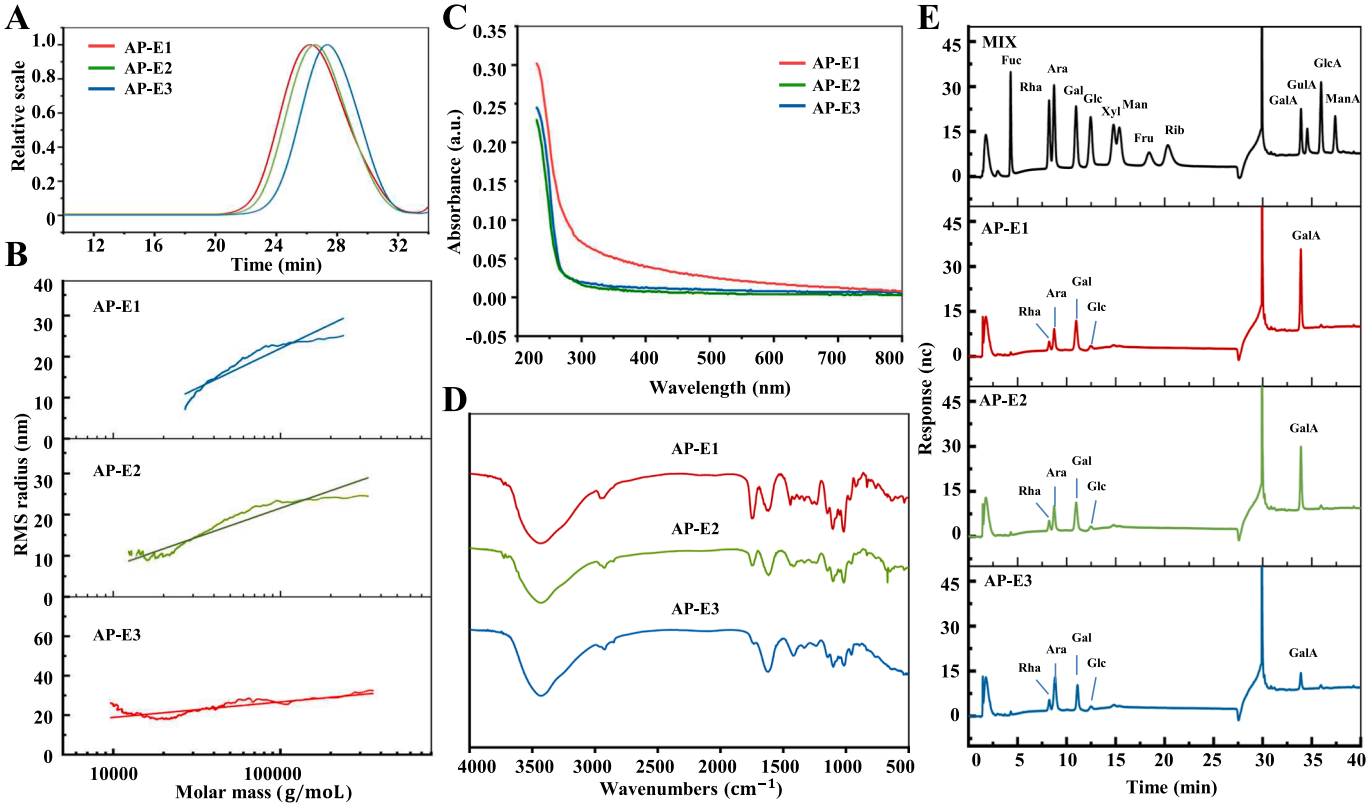

Fig. 1. Structural characterization of apple pectin with different degrees of esterification. SEC-MALLS-RI chromatograms (A), radius of gyration (B), UV spectrum (C), FT-IR spectrum (D), HPAEC spectrum (E) of AP-E1, AP-E2, and AP-E3. MIX, the mixed standard of monosaccharides; Fuc (Fucose); Rha (Rhamnose); Ara (Arabinose); Gal (Galactose); Glc (Glucose); Xly (Xylose); Man (Mannose); Fru (Fructose); Rib (Ribose); GalA (Galacturonic acid); GulA (Guluronic acid); GlcA (Glucuronic acid); and ManA (Mannuronic acid).

vibration and C–H asymmetric stretching vibration [5]. The presence of esterified and free carboxyl groups was indicated by the peaks observed at 1745 cm^{-1} and 1617 cm^{-1}, respectively [5]. Furthermore, the absorption band detected at 1420 cm^{-1} further confirmed the existence of pectic-polysaccharides [28]. Peaks ranging from 1200 cm^{-1} to 1000 cm^{-1} indicate the presence of C–O–C and C–C linkages within pectin molecules [29]. Additionally, the DE value of pectin can be calculated according to the FT-IR signals at 1745 cm^{-1} and 1617 cm^{-1}. As shown in Table 1, AP-E1 exhibited a DE value of 55.17 ± 1.85 %, classifying it as HMP polysaccharides. Notably, AP-E2 and AP-E3 had DE values of 36.36 ± 1.43 % and 5.08 ± 0.22 %, respectively, both classified as LMP polysaccharides. These results demonstrated that mild ultrasound-assisted alkali treatment significantly reduced the degree of esterification in pectin molecules. Our previous study also observed a reduction in the degree of esterification for alkali extracted polysaccharides [30].

3.1.4. Monosaccharide composition analysis

Chemical structures of pectin play a crucial role in determining their processing characteristics and biological functions. In order to gain insights into the chemical composition of AP-Es, we conducted an analysis and comparison of their monosaccharide units. As shown in Table 1 and Fig. 1E, AP-Es were found to contain Rha, Ara, Gal, Glc, and GalA. Typically, pectin polysaccharides consist primarily of GalA, Gal, Ara, Rha, and GlcA as the main monosaccharides [3]. The ratio can serve as an indicator for assessing the proportion of HG and RG-I pectic domains within pectin; likewise, the ratio of (Ara + Gal)/Rha reflects the branching chain length of RG-I [28]. In this study, we determined that the Rha/GalA value of AP-E1 and AP-E2 were 0.04 and 0.08, respectively; thus, suggesting that these samples predominantly consisted of HG rather than RG-I type backbones. Furthermore, AP-E3 had a significantly higher Rha/GalA value (0.22), indicating that it mainly comprised RG-I type pectin components. For AP-E1, it is likely that 73.86 % of the molar can be attributed to the HG region. With an increase in ultrasound-assisted alkali treatment time, the molar mass of the HG region decreased while the molar content of the RG-I region increased for AP-E2 and AP-E3. Specifically, for AP-E3, the molar content of the HG region was about 28.72 %, whereas the highly branched RG-I regions probably accounted for around 65.09 % molar content. This observation might be attributed to the elimination reactions causing molecular degradation and splitting of its HG backbone. Similarly, it was shown that that alkaline media treatment made the HG region susceptible to attack through elimination reactions [31]. The report of Cui et al. [32] demonstrated similar findings where alkali extraction disrupted the HG region and resulted in significant amounts of neutral sugar units attached to the RG-I backbone.

3.2. In vitro immunomodulatory activity of AP-Es

Macrophages typically phagocytose pathogens as the initial step in the human immune system's response, coordinating adaptive immune responses [33]. Consequently, phagocytosis plays a pivotal role in macrophage physiological function and enhances the body's immune resistance [34]. In this study, the immunomodulatory effects of AP with varying degrees of esterification on RAW 264.7 cells were investigated to identify the optimal AP for immunomodulatory. Before assessing the immunomodulatory activity of AP-Es on RAW 264.7 cells, MTT assays were employed to evaluate the cellular tolerance towards AP-Es. As shown in Fig. 2A, cell viability remained above 95 % after treatment with different concentrations of AP-Es, indicating a favorable tolerance profile of RAW 264.7 cells towards AP-Es. Furthermore, we investigated the impact of AP-Es on the release of NO, IL-6, and TNF-α in RAW 264.7 cells. Our findings demonstrated that all tested AP-Es activated RAW

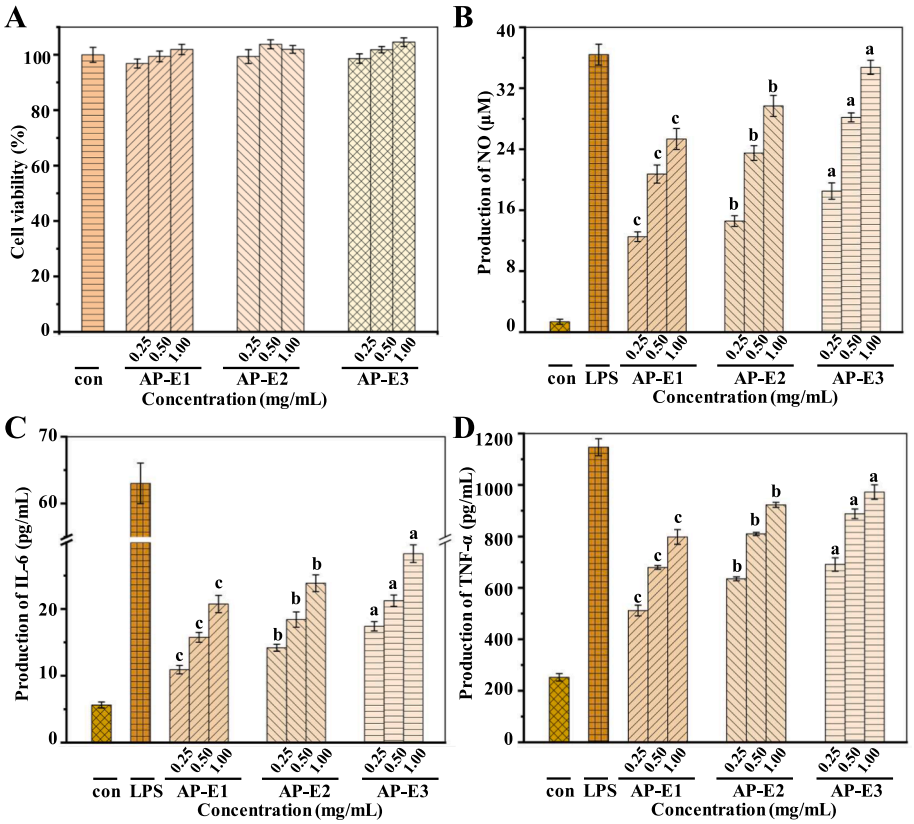

Fig. 2. *In vitro* immunomodulatory activity of apple pectin with different degrees of esterification. (A) Cytotoxicity of AP-E1, AP-E2, and AP-E3 on RAW 264.7 macrophages; (B–D) Effects of AP-E1, AP-E2, and AP-E3 on NO, IL-6, and TNF-α production in RAW 264.7 macrophages. NO (Nitric oxide); IL (Interleukin); TNF (Tumor necrosis factor).

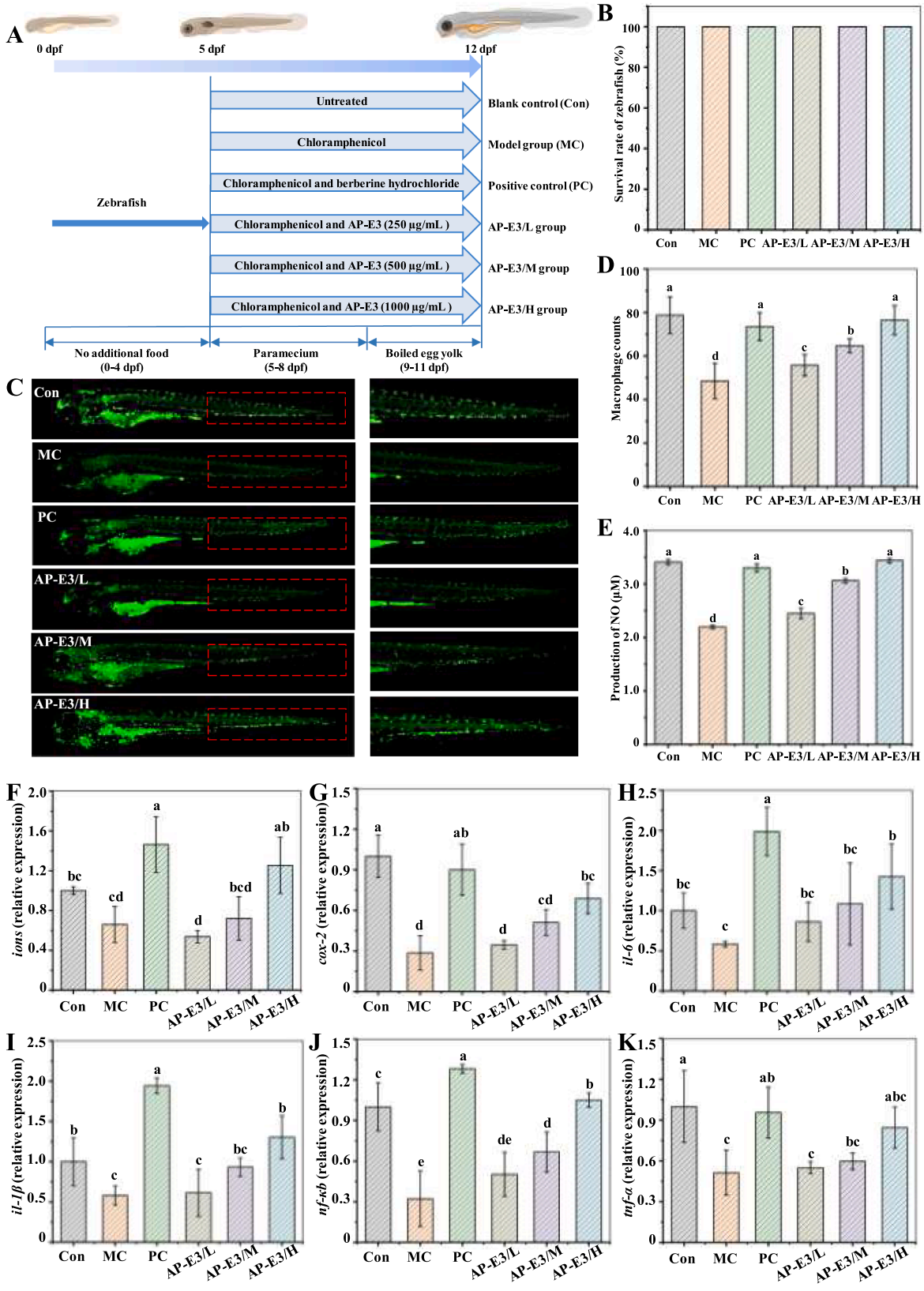

Fig. 3. AP-E3 increases macrophage numbers and mRNA expression of *inos*, *cox-2*, *il-6*, *il-1β*, *nf-κb*, and *tnf-α* genes in immunocompromised zebrafish. (A) Schematic flow of immunomodulatory activity in zebrafish. (B) Tolerance of zebrafish. (C–D) Photographs and number of fluorescent microspheres in zebrafish. (E) Effects of AP-E3 on NO production in zebrafish. (F–K) Effects of AP-E3 on the mRNA expression of *inos*, *cox-2*, *il-6*, *il-1β*, *nf-κb*, and *tnf-α* genes. *inos* (Inducible nitric oxide synthase); *cox-2* (Cyclooxygenase); *il* (Interleukin); *nf-κb* (Nuclear factor kappa B); *tnf* (Tumor necrosis factor).

264.7 cells and stimulated the secretion of NO, TNF-α, and IL-6. These results are consistent with our previous research, indicating the immunomodulatory effects of natural polysaccharides derived from apples [5]. Among all tested AP-Es at a dosage level up to 1.0 mg/mL (Fig. 2B, C, and D), AP-E3 exhibited the most significant effect. Specifically, production levels of NO were observed at 34.74 ± 0.93 μM, TNF-α at 972.69 ± 28.15 pg/mL, and IL-6 at 28.3 ± 1.33 pg/mL. The superior immunomodulatory ability of AP-E3 may be attributed to its lower esterification degree and distinctive structural properties such as molecular weight and monosaccharide composition. Overall, the present results indicated that AP-E3 can effectively enhance macrophage phagocytic ability, potentially improving innate immune responses. Subsequently, *in vivo* experiments using zebrafish were conducted to evaluate the immunomodulatory effects of AP-E3.

3.3. SAR analysis

The immunomodulatory capacity of AP-E3 of AP-E3 is closely associated with its structural properties. AP-E3 is a heteropolysaccharide composed of Ara, Rha, Gal, Glc, and GalA (Table 1). Previous studies have emphasized the ability of heteropolysaccharides to stimulate the secretion of NO and cytokines, thereby enhancing macrophage phagocytosis and overall immunomodulatory activity [35]. Furthermore, the immunoregulatory properties of polysaccharides are closely linked to their structural characteristics such as monosaccharide composition, M_w and glycosidic bond types [33,36,37]. In this study, AP-E3 exhibited a relatively low molecular weight of 22.17×10^3 Da, which is lower than that of the majority of reported apple pectin [38]. Previous studies have demonstrated that polysaccharides with lower molecular weights possess potent immunomodulatory activity by significantly enhancing macrophage phagocytosis and cytokine secretion ability [10]. Monosaccharide composition analysis revealed the presence of Ara, Rha, Gal, Glc, and GalA in AP-E3. Mild ultrasound-assisted alkali treatment significantly increased the molar ratios of Rha, Ara, and Gal as branched components. Notably, Gal is well-known for its immunomodulatory properties and polysaccharides with high Gal content from *Poria cocos* have exhibited remarkable immunoregulatory activities both *in vitro* and *in vivo* [39]. According to the findings reported by Du et al. [40], TLR2 exhibits a higher recognition affinity towards polysaccharides containing Gal, indicating a potent correlation between immunomodulatory activity and the presence of Gal. Furthermore, the monosaccharide composition analysis of AP-E3 revealed an abundance of the RG-I structural domain, which has been positively associated with the immunomodulatory activity of polysaccharide. It has been reported that the arabinogalactan structural motifs with RG-I might play a more pivotal role in immunomodulatory activity compared to HG [41]. In addition, it is well-known that branching regions in polysaccharides significantly contribute to their immunoregulatory activities and an elevated ratio of branched regions is often correlated with enhanced immunostimulatory effects [42]. The removal of branching regions has been demonstrated to reduce immunostimulatory activity and emphasizes the importance of the branching degree in the immunoregulatory function of polysaccharides [43].

3.4. In vivo immunomodulatory activity of AP-E3

3.4.1. AP-E3 restores macrophage numbers in immunocompromised zebrafish

Zebrafish exhibit significant similarities to mammals in both natural and acquired immune systems [44], making them valuable models for investigating *in vivo* immunomodulatory activities. The transparent larvae of zebrafish further enhance their utility in studying immune regulation by enabling direct observation of macrophage activity. These macrophages play a crucial role in early defense mechanisms such as pathogen phagocytosis and immune response regulation. In this study, zebrafish were utilized to evaluate the *in vivo* immunomodulatory effects of AP-E3. Before assessing the immunomodulatory activity of AP-E3 on zebrafish, we evaluated the tolerance of zebrafish to all drugs used. As shown in Fig. 3B, the survival rate of immunocompromised zebrafish treated with chloramphenicol (150 μg/mL) was 100 % after 24 h, demonstrating the model's applicability. Furthermore, zebrafish treated with berberine hydrochloride (5.33 μg/mL) and AP-E3 (0.25 − 1.0 mg/mL) also exhibited a survival rate of 100 %. These findings indicate that zebrafish display good tolerance towards both berberine hydrochloride and AP-E3.

Transgenic zebrafish expressing fluorescent macrophages were used to assess the impact of AP-E3 on macrophages, as illustrated in Fig. 3. The results (Fig. 3C and D) demonstrated a significantly reduced residual content of fluorescent microspheres in the MC group compared to the Con group, indicating successful establishment of the model with diminished macrophages population and impaired immune function in zebrafish. Remarkably, AP-E3 exhibited a pronounced ability to increase the number of fluorescent microspheres in zebrafish compared to the MC group, suggesting its potential for enhancing macrophage phagocytosis. Previous studies have substantiated that numerous polysaccharides can stimulate diverse immune cells such as macrophages, T cells, B cells, and DCs. This stimulation promotes cytokine release, activates the complement system, facilitates antibody generation, and exerts various regulatory roles within the immune system [45,46]. In the present study, alkali de-esterification of pectin enriched with RG-I structural domains resulted in an increased number of macrophages *in vivo* and exhibited significant immune activity. Furthermore, we investigated the impact of AP-E3 on NO release in zebrafish. NO serves as a crucial signaling molecule in immune cells, playing a pivotal role in signal transmission. It actively participates in immune cell resistance against invading pathogens and the proliferation of tumor cells while interacting with other cytokines and immune cells to promote the body's specific immune response [47]. As shown in Fig. 3E, all concentrations of AP-E3 effectively stimulated NO secretion/release from zebrafish. Among these doses, 1.0 mg/mL demonstrated the most pronounced effect without any significant different compared to the control and positive groups. Notably, AP-E3 exhibited superior ability over other active polysaccharides to enhance macrophage NO secretion possibly due to its distinctive structural features.

3.4.2. AP-E3 upregulates the mRNA expression of *tnf-α, il-1β, il-6, cox-2, inos, and nf-κb* genes

The effect of AP-E3 on the expression of g immune-related genes in zebrafish was assessed by performing real-time qPCR analysis on RNA isolated from zebrafish. The effects of AP-E3 on the mRNA expression of *tnf-α*, *il-1β*, *il-6*, *cox-2*, *inos*, and *nf-κb* genes in zebrafish are illustrated in Fig. 3F − K. In comparison to the untreated control group the model group of zebrafish exhibited significantly reduced expression of these genes, indicating the effectiveness of chloramphenicol as an immunosuppressive drug. In contrast, treatment with berberine hydrochloride and various concentrations of AP-E3 resulted in up-regulation of these genes to varying extents. Notably, the expression of these genes exhibited a dose-dependent response to AP-E3. Specifically, treatment with 1.0 mg/mL of AP-E3 resulted in up-regulation of *tnf-α*, *il-1β*, *il-6*, *cox-2*, *inos*, and *nf-κb* genes by 1.64-, 2.25-, 2.45-, 2.40-, 1.89-, and 3.28-fold, respectively, compared to the model group. Both *cox-2* and *inos* are recognized as important inflammatory mediators and *inos* is primarily responsible for promoting NO synthesis in macrophages, while overexpression can enhance NO production and induce *cox-2* expression [48]. Moreover, *tnf-α*, *il-1β*, and *il-6* are widely considered as pivotal pro-inflammatory cytokines. *tnf-α*, predominantly synthesized by activated macrophages, plays a critical role in stimulating the production and secretion of diverse immune modulators and inflammatory cytokines [49]. Furthermore, *il-1β* and *il-6* are implicated in triggering acute immune responses that result in fever [49]. Additionally, Ikeda-Ohtsubo et al. [50] demonstrated that fucoidan derived from Okinawa mozuku (*Cladosiphon okamuranus*) treatment modulated the relative expression

of innate immunity genes in zebrafish larval such as *il-1β*, *il-10*, and *tnf-α*. Collectively, real-time qPCR analysis revealed that AP-E3 up-regulated the expression of immune-related genes in zebrafish in a dose-dependent manner, thereby demonstrating the immunomodulatory potential of AP-E3.

3.4.3. *AP-E3/H restores microbial community homeostasis in immunocompromised zebrafish*

To evaluate the impact of AP-E3/H ingestion on the zebrafish gut microbiota, we employed 16S rRNA gene sequencing to analyze its composition. The results from α-diversity analysis (Table S2, Fig. 4A and B) revealed that chloramphenicol had no significant effect on the Chao and Ace indices of gut microorganisms; however, it significantly reduced the Shannon and Simpson indices, indicating a decrease in the community diversity of zebrafish gut microorganisms. Conversely, treatment with AP-E3/H resulted in an enhancement of community diversity within zebrafish gut microorganisms. Changes in diversity serve as crucial indicator for assessing community stability, with higher diversity and complex community structure reflecting greater stability. Therefore, compared to the MC group, AP-E3/H restored homeostasis within the gut microbial community of immunosuppressed zebrafish. The PCoA analysis clearly demonstrated distinct separation of the gut microbiota composition among the Con, MC, and AP-E3/H groups (Fig. 4C), highlighting t the significant impact of both chloramphenicol treatment and AP-E3/H therapy on gut microbiota composition. Additionally, the Venn diagram revealed a lower number of ASVs in the MC group (107 ASVs)

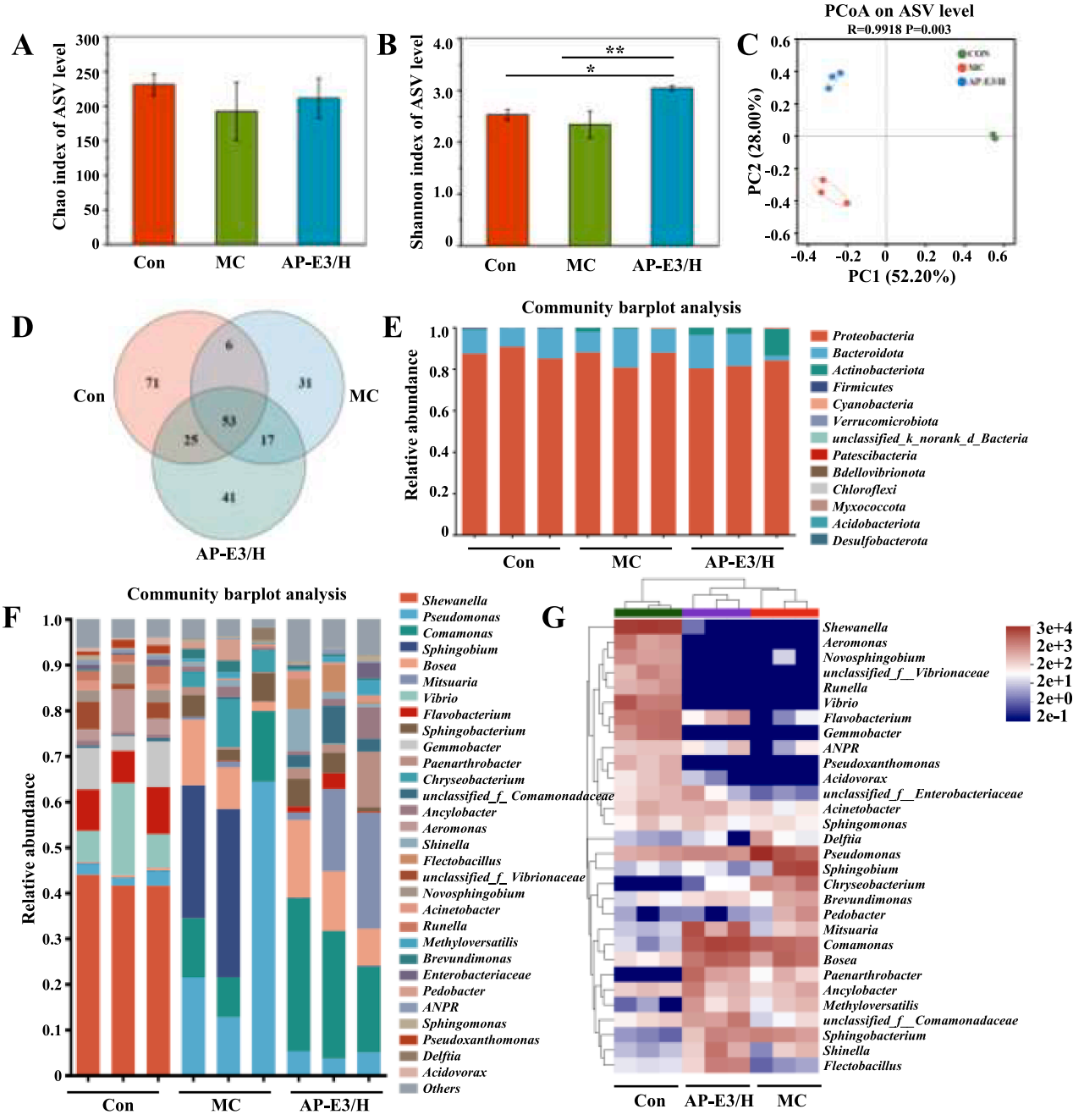

Fig. 4. AP-E3 restores microbial community homeostasis in immunocompromised zebrafish. (A–B) Chao and Shannon index values ($0.01 < p \leq 0.05$ marked for *, $p \leq 0.01$ marked for **). (C) PCoA score plot of gut microbiota at ASV level. (D) Venn diagram. (E–F) Taxonomic composition of gut microbiota at phylum and genus level. (G) Cluster analysis of the relative abundance of microbial community at the genus level (Top 30). Different colors represent the relative expression of metabolites in the samples.

compared to the Con group (155 ASVs) (Fig. 4D). Conversely, restoration of OTUs (136 ASVs) was observed in the AP-E3/H treatment group.

At the phylum level, the dominant bacterial communities consisted mainly of *Proteobacteria*, *Bacteroidota*, *Actinobacteriota*, and *Firmicutes*, with *Proteobacteria* and *Bacteroidota* being the most prevalent without any differences observed (Fig. 4E). The developmental stages of zebrafish encompass larval, juveniles and adults. Throughout all stages of the zebrafish life cycle, members belonging to the phylum *Proteobacteria* dominate the gut microbiota [14,51], which is consistent with our findings. At the genus level, analysis revealed higher relative abundances in the Con group for *Shewanella*, *Flavobacterium*, *Gemmobacter*, *Vibrio*, *Pseudomonas*, and *Aeromonas* (Fig. 4F). In contrast, the MC group exhibited increased abundance of *Pseudomonas*, *Comamonas*, *Sphingobium*, and *Bosea*. The AP-E3/H group showed higher abundances of *Pseudomonas*, *Comamonas*, *Flavobacterium*, *Sphingobium*, *Bosea*, and *Mitsuaria*. Some studies have demonstrated that bacterial populations in the mouth, pharynx, esophagus, and proximal intestine of zebrafish increase from mouth opening untill 4 dpf, followed by an increase in gut microbiota abundance between 4 and 8 dpf. *Aeromonas* and *Pseudomonas* species are predominant during embryo and larvae [51], while *Fusobacteria* are more prevalent during adulthood [52].

The immune system interacts with the gut microbiota and exerts an influence on host health by modulating the composition and diversity of the microbiota [53]. Cluster analysis revealed a significant reduction in the abundance of *Shewanella*, *Aeromonas*, *Novosphingobium*, *unclassified_Vibrionaceae*, *Runella, Vibrio*, *Flavobacterium*, *Gemmobacter*, *Allorhizobium-Neorhizobium-Pararhizobium-Rhizobium* (*ANPR*), *Pseudoxanthomonas*, *Acidovorax*, *unclassified_f Enterobacteriaceae*, and *Acinetobacter* in the MC group (Fig. 4G). This suggests that chloramphenicol as an antibiotic may have induced dysbiosis in zebrafish microbiota. The treatment with AP-E3/H resulted in the restoration of *Flavobacterium, ANPR*, and *Acinetobacter* while no significant changes were observed in other bacteria. *Flavobacterium* is a Gram-negative bacterium known to elicit innate immune responses in zebrafish [54], particularly activating neutrophils and macrophages, thereby enhancing the host's defense mechanisms [55]. *Acinetobacter*, predominantly present in the zebrafish gut microbiota, interacts with the host immune system and influence the expression of immune genes in the intestine. This bacterium, along with other gut microbes, plays a crucial role in regulating the immune balance and augmenting host's resistance against pathogens. Previous studies have demonstrated that *Acinetobacter* can enhance the expression of immune genes, thereby contributing to a robust immune response in zebrafish [56]. Furthermore, the abundance of *Sphingobium*, *Chryseobacterium, Brevundimonas, Pedobacter, Mitsuaria, Comamonas, Bosea, Paenarthrobacter, Methyloversatilis,* and *Sphingobacterium* was significantly induced in the MC group. However, after AP-E3/H treatment, only *Sphingobium*, *Chryseobacterium,* and *Pedobacter* showed significant restoration while no notable changes were observed in other bacterial taxa. Notably though polysaccharides were found to have no significant impact on the microbiota composition of zebrafish larvae [50]. Our findings suggest that AP has potential for selectively restoring gut microbial homeostasis and improving immunosuppressed zebrafish.

3.4.4. AP-E3/H restores metabolic homeostasis in immunocompromised zebrafish

Metabolites play a crucial role in regulating immune responses, exerting specific effects on the function and activity of immune cells, thereby influencing overall immune regulation [57]. In this study, we performed non-targeted metabolite profiling to investigate changes in intestinal metabolites following AP-E3/H intervention and elucidate the mechanisms underlying its immunomodulatory effects in immunocompromised zebrafish. As illustrated in Fig. 5A, a total of 1018 metabolites were identified and classified into various groups based on the HMDB database classification, including lipids and lipid-like molecules (367; 36.05 %), organic acids and derivatives (193; 18.96 %), organoheterocyclic compounds (142; 13.95 %), organic oxygen compounds (56; 8.81 %), and benzenoids (64; 6.29 %). The Venn diagram in Fig. 5B displayed the counts of differentially expressed metabolites in response to chloramphenicol or AP-E3/H treatment using criteria of VIP score $>$ 1.0, $p < 0.05$, and $|\log_2 FC| \geq 0$. Among these 455 differential metabolites, a total of 68 consistently exhibited alterations across comparison groups including AP-E3/H versus MC, AP-E3/H versus Con, and MC versus Con. The PLS-DA score plots (Fig. 5C) based on zebrafish metabolite abundance revealed distinct clustering patterns for the Con, MC, and AP-E3/H samples. The volcano plots depicted in Fig. 5D and F visually highlighted significant shifts in metabolite levels. In the comparison between the MC control group and the Con group, a substantial number of metabolites displayed significant downregulation, indicating pronounced metabolic disturbances in the MC group. The comparison between the AP-E3/H treated group and the MC group reveals a significant increase in upregulated metabolites and a decrease in downregulated metabolites, indicating that AP-E3/H treatment effectively alleviates the observed metabolic disruptions observed in the MC group. Evaluation of the AP-E3/H treated group relative to the Con group suggests that although some metabolites remain significantly altered, there is an overall trend towards normalization of the metabolic profile closer to that of the control group. These findings underscore that the potential of AP-E3/H treatment in restoring disrupted metabolic homeostasis caused by chloramphenicol.

Cluster analysis of the top 30 differential metabolites in zebrafish is presented in Fig. 5G. In the MC group, significant upregulation was observed for metabolites such as minodronic acid, chloramphenicol, LysoPC(20:4(5Z,8Z,11Z,14Z)/0:0), LysoPC (20:4(8Z,11Z,14Z,17Z)/0:0), and PC (20:5/0:0). However, treatment with AP-E3/H markedly reduced their levels. Notably, immunosuppressive agent chloramphenicol decreased in the AP-E3/H treated group due to enhanced metabolism and excretion facilitated by polysaccharides. Previous studies have reported that polysaccharides can modulate metabolic pathways and enhance liver function promote drug metabolism and excretion [58,59]. These findings suggest that AP-E3/H may mitigate chloramphenicol's immunosuppressive effects by promoting its clearance and potentially enhancing immune function in zebrafish. The analysis of Fig. 5G also demonstrates a significant downregulation in metabolites within the MC group, including uric acid, 1-stearoylglycerophosphoserine, dodecylbenzenesulfonic acid, oxymetholone, docosahexaenoic acid (DHA), (+/-)10-HDoHE, and several phosphatidylcholine (PC) metabolites. Notably, DHA, (+/-)10-HDoHE, and PC-related metabolites that are crucial for immune modulation and cellular metabolism exhibited remarkable reductions. These metabolites are typically associated with cell membrane functionality and signal transduction while playing a substantial role in immune function [60]. Treatment with AP-E3/H significantly upregulated these metabolites, suggesting its potential to activate suppressed signaling pathways and enhance the production of these critical compounds. This indicates that AP-E3/H can restore or enhance compromised immune and metabolic functions. DHA and its metabolites are recognized for their significant roles in modulating immune cell activity, cytokine production, anti-inflammatory processes, and enhancing immune function [61]. The significant increase in DHA levels following AP-E3/H treatment suggests a restoration of these beneficial effects. Moreover, the upregulation of PC-related metabolites implies an improvement in cell membrane integrity and signaling, essential for effective immune responses [62].

Fig. 6 illustrates the results of KEGG enrichment analysis and differential abundance scores, demonstrating significant alterations in metabolic pathways. In the MC versus Con comparison, notable downregulations were observed in pathways such as retrograde endocannabinoid signaling, arachidonic acid metabolism, glycerophospholipid metabolism, Fc gamma R-mediated phagocytosis, AMPK signaling, and neuroactive ligand-receptor interaction, indicating metabolic disruptions in the MC group. The AP-E3/H versus MC comparison reveals that AP-E3/H treatment restores metabolic functions by upregulating these pathways. Furthermore, when comparing AP-E3/H with Con

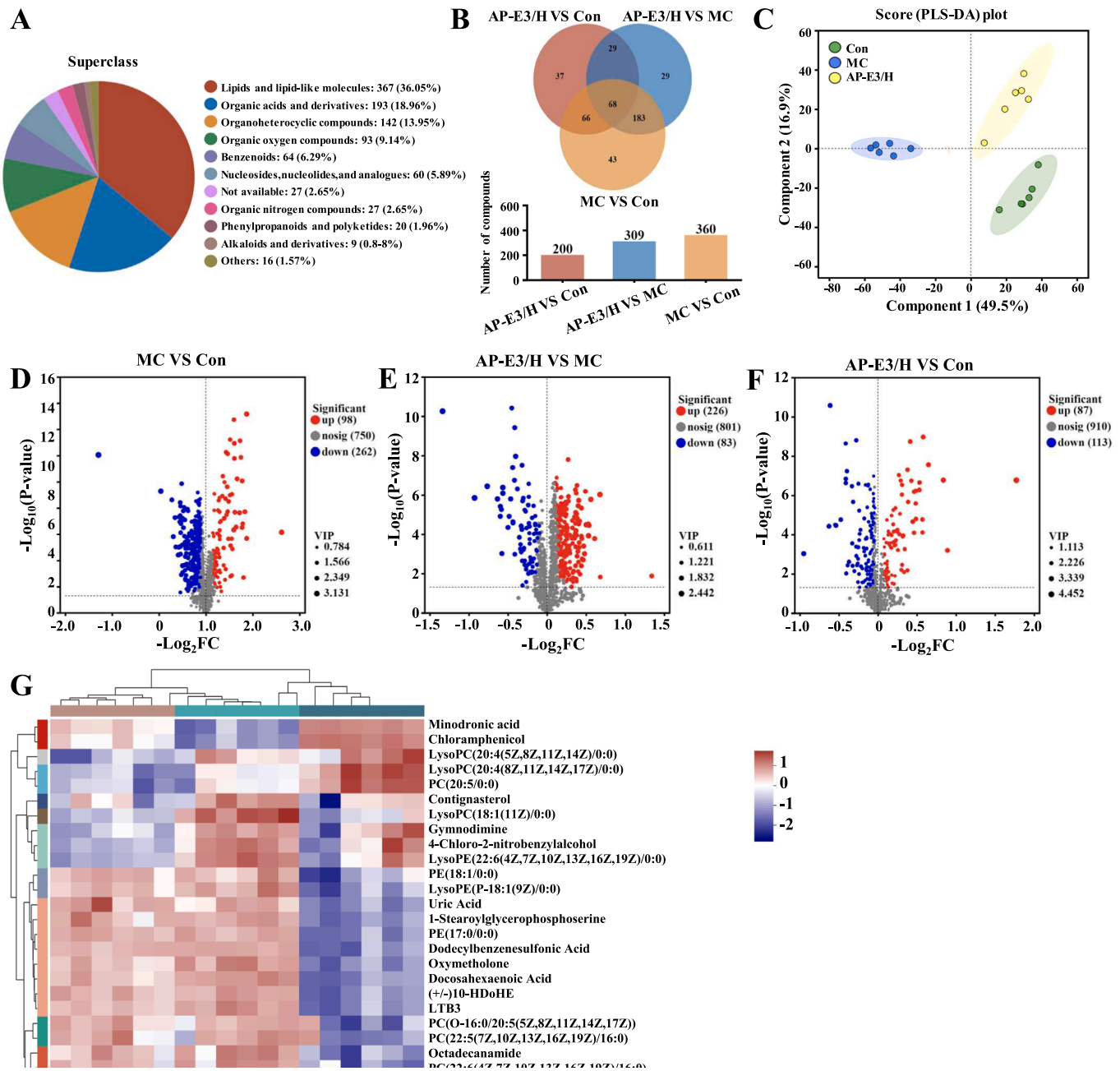

Fig. 5. AP-E3 restores metabolic homeostasis in immunocompromised zebrafish. (A) Pie chart illustrating metabolite counts annotated in the HDMB database at the superclass level. (B) Venn diagram displaying the differentially expressed metabolites specific or common among different comparison groups. (C) PLS-DA score plot of metabolites. (D–F) Volcano plots showcasing significant shifts in metabolite levels. (G) Cluster analysis of relative expression of differential metabolites (Top 30).

comparison, AP-E3/H treatment significantly impacts pathways including retrograde endocannabinoid signaling, arachidonic acid metabolism, glycerophospholipid metabolism, neuroactive ligand-receptor interaction and NF-κB signaling, highlighting its role in modulating immune-related and metabolic pathways and restoring metabolic balance. So, metabolomics analysis demonstrated that AP-E3/H treatment restores the production of metabolites involved in various metabolic pathways related to signaling, metabolism, and the immune system. This suggests that polysaccharides can help restore metabolic balance and improve immune responses for overall immune recovery in immunocompromised zebrafish.

We further investigated the correlation between metabolites and microorganisms, as shown in Fig. 7A. *Pseudomonas, Parasediminibacterium,* and *Aeromonas* exhibited a negative correlation with most metabolites. Conversely, *Shewanella, Flavobacterium, Chryseobacterium, Sphaerotilus, unclassified_f_Comamonadaceae, Acidovorax, Pseudoxanthomonas, Novosphingobium* showed a positive correlation with most metabolites, particularly phosphatidylcholine and DHA along with their related metabolites. According to Fig. 4G, treatment with chloramphenicol resulted in a reduction in the abundance of *Shewanella, Flavobacterium, Chryseobacterium, Sphaerotilus, unclassified_f_Comamonadaceae, Acidovorax, Pseudoxanthomonas*, and *Novosphingobium*, thus highlighting the potential influence of chloramphenicol on gut microbiota diversity. Furthermore Fig. 7A suggests that these bacteria are positively associated with phosphatidylcholine, docosahexaenoic acid and their related metabolites, suggesting their crucial role in the metabolism of these important immunomodulatory molecules. In addition to its direct impact on bacterial growth, chloramphenicol also exerts an

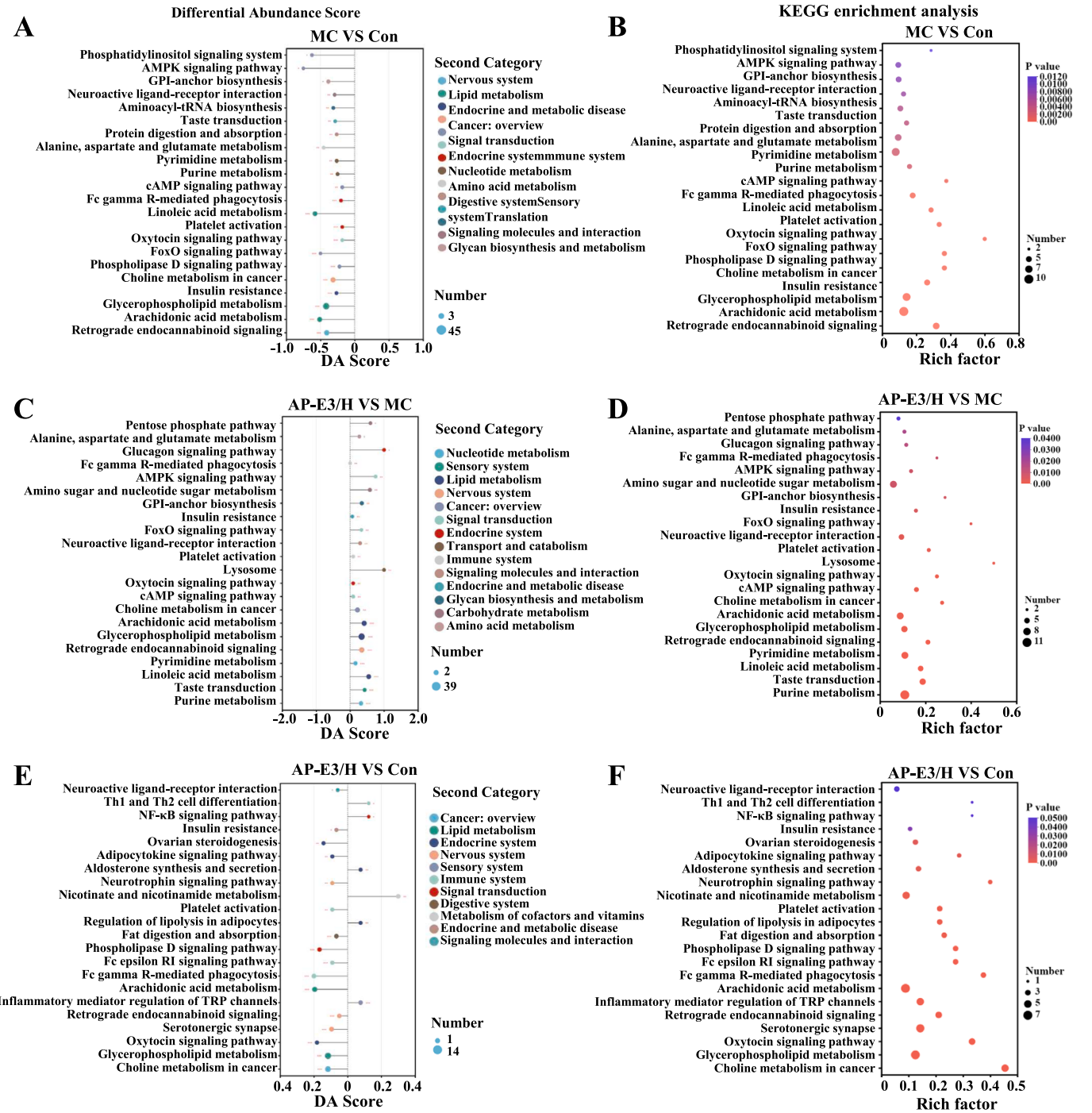

Fig. 6. KEGG enrichment analysis and differential abundance Score of differential metabolites. (A, C, E) Differential abundance score of differential metabolites in various comparison groups. The horizontal coordinate is the rich factor and the vertical coordinate is the KEGG pathway. The size of the bubbles represents the number of metabolites enriched in the corresponding pathway, and the color of the bubbles represents the magnitude of the significance *p*-value. (B, D, F) KEGG enrichment analysis of differential metabolites in various comparison groups (MC versus Con, AP-E3/H versus MC, and AP-E3/H versus Con). The horizontal axis shows the differential abundance score (DA score) and the vertical axis represents KEGG metabolic pathways. A DA score of "1″ indicates up-regulation of all annotated differential metabolites in the pathway, and "-1" indicates down-regulation. Line length shows the absolute DA score, and dot size indicates the number of differential metabolites in the pathway.

indirect influence on host immune function through alterations in key metabolic products and microbial community structure. In contrast, AP has demonstrated the ability to restore gut microbiota and metabolic balance in chloramphenicol-induced immunocompromised zebrafish. Fig. 7B provides a summary of the effects of AP on chloramphenicol-induced immunocompromised zebrafish. Functioning as a prebiotic, AP facilitates the growth of beneficial bacteria, thereby enhancing the production of essential immunomodulatory metabolites. This restoration of microbial balance and metabolite production aids in reestablish immune function and metabolic homeostasis, underscoring the potential utility of AP in mitigating the deleterious impacts of antibiotics on gut microbiota and host immunity.

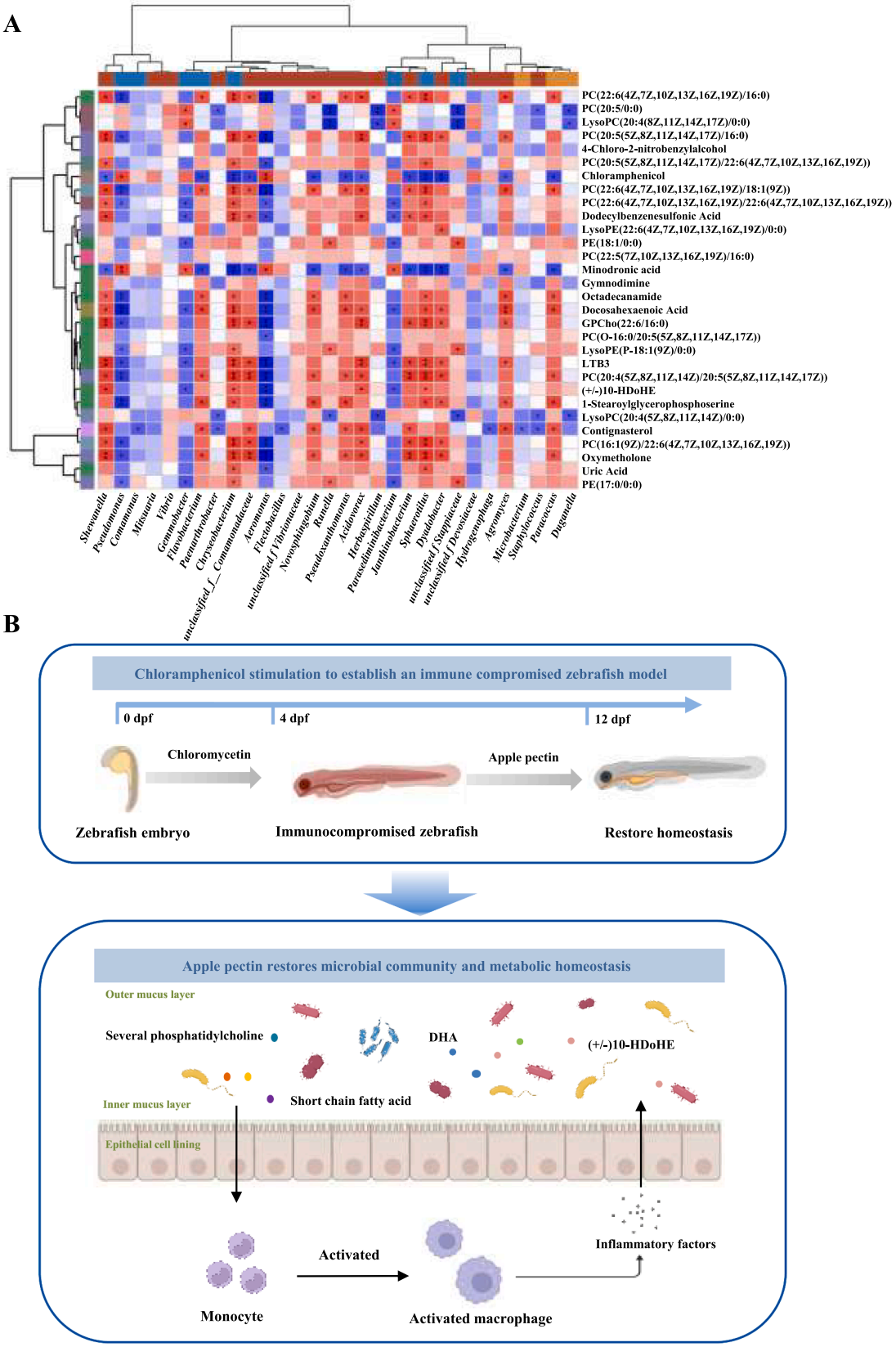

Fig. 7. Correlation analysis and immunoregulatory mechanisms. (A) Microbiota-metabolism related heat map. (B) Schematic mechanism of the effect of apple pectin on chloramphenicol-induced immunocompromised zebrafish.

4. Conclusion

In this study, we investigated the impact of mild ultrasound-assisted alkali treatment on the esterification degree of AP and its subsequent impact on immunomodulatory activity. AP with varying degrees of esterification were successfully synthesized and characterized, revealing a reduction in HG domains and an increase in RG-I domains as the esterification decreased. Among these samples, AP-E3, which exhibited the lowest degree of esterification and the highest RG-I content, displayed significantly enhanced immunomodulatory activity in RAW 264.7 cells. Using transgenic zebrafish models with fluorescent macrophages, AP-E3 demonstrated a dose-dependent increase in macrophage counts. Further experiments using wild-type zebrafish (AB strain) revealed that AP-E3 upregulated key immune-related genes such as *tnf-α*, *il-1β*, *il-6*, *cox-2*, *inos*, and *nf-κb*, thereby improving the gut microbiota composition and abundance in chloramphenicol-induced immunosuppressed zebrafish. Metabolomics analysis indicated that AP-E3 facilitated restoration of metabolic homeostasis by activating various signaling pathways involved in immune response and metabolism. Our study demonstrates that the immunomodulatory activity of AP can be significantly enhanced by reducing its esterification degree and increasing its RG-I content through mild ultrasound-assisted alkali treatment. This research provides valuable insights into the AP's SAR, suggesting potential applications for immune enhancement and gut health maintenance. In future work, we will utilize a germ-free zebrafish model to further investigate the key targets of gut microbiota in regulating the immune system of zebrafish.

CRediT authorship contribution statement

Huan Guo: Writing – review & editing, Writing – original draft, Methodology, Investigation, Conceptualization. **Dong Li:** Software, Investigation. **Baohe Miao:** Writing – review & editing, Funding acquisition. **Kanglin Feng:** Investigation. **Guijing Chen:** Writing – review & editing. **Renyou Gan:** Writing – review & editing. **Zhiliang Kang:** Writing – review & editing. **Hong Gao:** Writing – review & editing, Supervision, Funding acquisition, Conceptualization.

Declaration of competing interest

The authors declare that they have no known competing financial interests or personal relationships that could have appeared to influence the work reported in this paper.

Acknowledgments

This work was financially supported by the National Natural Science Foundation of China (No. 32072321), the Sichuan University and Luzhou City Strategic Cooperation Project (no. 2019CDLZ-20), the Liangshan Prefecture Technology Plan in 2021 (21ZDYF0052), the Agricultural Science and Technology Innovation of Chinese Academy of Agricultural Sciences (ASTIP2024-34-IUA-05), and the Local Financial Funds of National Agricultural Science and Technology Center (NASC2021PC02).

Appendix A. Supplementary data

Supplementary data to this article can be found online at https://doi.org/10.1016/j.ultsonch.2024.107215.

References

[1] Y. Jiang, J. Du, Properties of high-methoxyl pectin extracted from "Fuji" apple pomace in China, J. Food Process Eng. 40 (2016) 1–11.
[2] D. Mohnen, Pectin structure and biosynthesis, Curr. Opin. Plant Biol. 11 (2008) 266–277.
[3] W. Tang, D. Liu, J.Q. Wang, X.J. Huang, J.Y. Yin, F. Geng, S.P. Nie, Isolation and structure characterization of a low methyl-esterified pectin from the tuber of *Dioscorea opposita* Thunb, Food Chem. 359 (2021) 129899.
[4] I. Calvete-Torre, C. Sabater, M.J. Antón, F.J. Moreno, S. Riestra, A. Margolles, L. Ruiz, Prebiotic potential of apple pomace and pectins from different apple varieties: Modulatory effects on key target commensal microbial populations, Food Hydrocolloid. 133 (2022) 107958.
[5] H. Guo, H. Li, W. Ran, W. Yu, Y. Xiao, R. Gan, H. Gao, Structural and functional characteristics of pectins from three cultivars of apple (*Malus pumila* Mill.) pomaces, Int. J. Biol. Macromol. 269 (2024) 132002.
[6] W.L. Liang, J.S. Liao, J.R. Qi, W.X. Jiang, X.Q. Yang, Physicochemical characteristics and functional properties of high methoxyl pectin with different degree of esterification, Food Chem. 375 (2022) 131806.
[7] W. Li, J. Li, J. Wang, Y. He, Y.C. Hu, D.T. Wu, L. Zou, Effects of various degrees of esterification on antioxidant and immunostimulatory activities of okra pectic-polysaccharides, Front. Nutr. 9 (2022) 1025897.
[8] W.B. Li, J. Wang, M.M. Qu Mo, J. Li, M. Li, Y. Liu, S. Wang, Y.C. Hu, L. Zou, D. T. Wu, Pectic polysaccharides from Tartary buckwheat sprouts: Effects of ultrasound-assisted Fenton treatment and mild alkali treatment on their physicochemical characteristics and biological functions, Ultrason. Sonochem. 109 (2024) 107014.
[9] L. Fan, S. Zuo, H. Tan, J. Hu, J. Cheng, Q. Wu, S. Nie, Preventive effects of pectin with various degrees of esterification on ulcerative colitis in mice, Food Funct. 11 (2020) 2886–2897.
[10] W.B. Li, J. Lei, M.M. Qu Mo, J. Li, J. Wei, Y. Liu, S. Wang, Y.C. Hu, L. Zou, D.T. Wu, Impacts of ultrasound-assisted Fenton degradation and alkaline de-esterification on structural properties and biological effects of pectic polysaccharides from Tartary buckwheat leaves, Ultrason. Sonochem. 106 (2024) 106895.
[11] J. Li, J. Feng, X. Luo, M.M. Qu Mo, W.B. Li, J.W. Huang, S. Wang, Y.C. Hu, L. Zou, D.T. Wu, Potential structure-function relationships of pectic polysaccharides from quinoa microgreens: Impact of various esterification degrees, Food Res. Int. 187 (2024) 114395.
[12] H. Xia, H. Chen, X. Cheng, M. Yin, X. Yao, J. Ma, M. Huang, G. Chen, H. Liu, Zebrafish: an efficient vertebrate model for understanding role of gut microbiota, Mol. Med. 28 (2022) 161.
[13] H. Lu, P. Li, X. Huang, C.H. Wang, M. Li, Z.Z. Xu, Zebrafish model for human gut microbiome-related studies: advantages and limitations, Med. Microecol. 8 (2021) 100042.
[14] A. Lopez Nadal, W. Ikeda-Ohtsubo, D. Sipkema, D. Peggs, C. McGurk, M. Forlenza, G.F. Wiegertjes, S. Brugman, Feed, microbiota, and gut immunity: using the zebrafish model to understand fish health, Front. Immunol. 11 (2020) 114.
[15] K.A.G. Michel Dubois, J.K. Hamilton, P.A. Rebers, And Fred Smith, Colorimetric method for determination of sugars and related substances, Anal. Chem. 28 (1956) 350–356.
[16] N. Blumenkrantz, Asboe-Hansen, New method for quantitative determination of uronic acids, Anal. Biochem. 54 (1973) 484–489.
[17] M.M. Bradford, A rapid and sensitive method for the quantitation of microgramquantities of protein utilizing the principle of protein-dye binding, Anal. Biochem. 72 (1976) 248–254.
[18] Z.F. Zhang, G.Y. Lv, T.T. Song, Z.W. Xu, M.Y. Wang, Effects of different extraction methods on the structural and biological properties of *Hericium coralloides* polysaccharides, Food Chem. 445 (2024) 138752.
[19] Z. Mao, L. Yang, Y. Lv, Y. Chen, M. Zhou, C. Fang, B. Zhu, F. Zhou, Z. Ding, A glucuronogalactomannan isolated from *Tetrastigma hemsleyanum* Diels et Gilg: Structure and immunomodulatory activity, Carbohyd. Polym. 333 (2024) 121922.
[20] C.P.A.K. Chatjigakis, N. Proxeniab, O. Kalantzib, P. Rodisb, M. Polissiou, FT-IR spectroscopy as a tool for measuring degree of methyl esterification in pectins isolated from ripening papaya fruit, Carbohyd. Polym. 37 (1998) 395–408.
[21] F. Xiao, W. Zhu, Y. Yu, Z. He, B. Wu, C. Wang, L. Shu, X. Li, H. Yin, J. Wang, P. Juneau, X. Zheng, Y. Wu, J. Li, X. Chen, D. Hou, Z. Huang, J. He, G. Xu, L. Xie, J. Huang, Q. Yan, Host development overwhelms environmental dispersal in governing the ecological succession of zebrafish gut microbiota, NPJ Biofilms Microbi. 7 (2021) 5.
[22] H. Guo, Y. Du, H. Gao, Y. Liao, H. Liu, D. Wu, R. Gan, H. Gao, Isolation, purification, degradation of citrus pectin and correlation between molecular weight and their biological properties, LWT - Food Sci. Technol. 196 (2024) 115837.
[23] S. Wei, C. Wang, Q. Zhang, H. Yang, E.C. Deehan, X. Zong, Y. Wang, M. Jin, Dynamics of microbial communities during inulin fermentation associated with the temporal response in SCFA production, Carbohyd. Polym. 298 (2022) 120057.
[24] A. Chen, Y. Liu, T. Zhang, Y. Xiao, X. Xu, Z. Xu, H. Xu, Chain conformation, mucoadhesive properties of fucoidan in the gastrointestinal tract and its effects on the gut microbiota, Carbohyd. Polym. 304 (2023) 120460.
[25] T. Kato, T. Okamoto, T. Tokuya, A. Takahashi, Solution properties and chain flexibility of pullulan in aqueous solution, Biopolymers 21 (1982) 1623–1633.
[26] J.K. Yan, J.J. Pei, H.L. Ma, Z.B. Wang, Effects of ultrasound on molecular properties, structure, chain conformation and degradation kinetics of carboxylic curdlan, Carbohyd. Polym. 121 (2015) 64–70.
[27] D.T. Wu, Y.X. Zhao, Q. Yuan, S. Wang, R.Y. Gan, Y.C. Hu, L. Zou, Influence of ultrasound assisted metal-free Fenton reaction on the structural characteristic and immunostimulatory activity of a beta-d-glucan isolated from Dictyophora indusiata, Int. J. Biol. Macromol. 220 (2022) 97–108.
[28] Y. Song, J. Lei, J. Li, J. Wang, J.L. Hu, X.Q. Zheng, Y.C. Hu, L. Zou, D.T. Wu, Structural properties and biological activities of soluble dietary fibers rich in pectic-polysaccharides from different buckwheat green leaves, Int. J. Biol. Macromol. 253 (2023) 126686.

[29] A. Wikiera, A. Koziol, M. Mika, B. Stodolak, Structure and bioactivity of apple pectin isolated with arabinanase and mannanase, Food Chem. 388 (2022) 133020.
[30] H. Guo, M.X. Fu, Y.X. Zhao, H. Li, H.B. Li, D.T. Wu, R.Y. Gan, The chemical, structural, and biological properties of crude polysaccharides from sweet tea (*Lithocarpus litseifolius* (Hance) Chun) based on different extraction technologies, Foods 10 (2021) 1779.
[31] W. Hu, S. Chen, D. Wu, J. Zheng, X. Ye, Ultrasonic-assisted citrus pectin modification in the bicarbonate-activated hydrogen peroxide system: Chemical and microstructural analysis, Ultrason. Sonochem. 58 (2019) 104576.
[32] J. Cui, W. Ren, C. Zhao, W. Gao, G. Tian, Y. Bao, Y. Lian, J. Zheng, The structure-property relationships of acid- and alkali-extracted grapefruit peel pectins, Carbohyd. Polym. 229 (2020) 115524.
[33] Q.Y. Ma, Q.D. Xu, N. Chen, W.C. Zeng, A polysaccharide from *Epiphyllum oxypetalum* (DC.) Haw. and its immunomodulatory activity, Int. J. Biol. Macromol. 253 (2023) 126792.
[34] S. Gordon, Phagocytosis: an immunobiologic process, Immunity 44 (2016) 463–475.
[35] I.A. Schepetkin, G. Xie, L.N. Kirpotina, R.A. Klein, M.A. Jutila, M.T. Quinn, Macrophage immunomodulatory activity of polysaccharides isolated from *Opuntia polyacantha*, Int. Immunopharmacol. 8 (2008) 1455–1466.
[36] X.L. Ji, J.H. Guo, J.Y. Tian, K. Ma, Y.Q. Liu, Research progress on degradation methods and product properties of plant polysaccharides, J. Light Ind. 38 (2023) 55–62.
[37] X. Ji, C. Hou, Y. Gao, Y. Xue, Y. Yan, X Guo, Metagenomic analysis of gut microbiota modulatory effects of jujube (*Ziziphus jujuba* Mill.) polysaccharides in a colorectal cancer mouse model. Food Funct. 11(2020) 163–173.
[38] B.E. Morales-Contreras, L. Wicker, W. Rosas-Flores, J.C. Contreras-Esquivel, J. A. Gallegos-Infante, D. Reyes-Jaquez, J. Morales-Castro, Apple pomace from variety "Blanca de Asturias" as sustainable source of pectin: Composition, rheological, and thermal properties, LWT - Food Sci. Technol. 117 (2020) 108641.
[39] L. Huang, M. Shen, G.A. Morris, J. Xie, Sulfated polysaccharides: Immunomodulation and signaling mechanisms, Trends Food Sci. Technol. 92 (2019) 1–11.
[40] J. Du, J. Li, J. Zhu, C. Huang, S. Bi, L. Song, X. Hu, R. Yu, Structural characterization and immunomodulatory activity of a novel polysaccharide from *Ficus carica*, Food Funct. 9 (2018) 3930–3943.
[41] H. Kim, B.S. Kwak, H.D. Hong, H.J. Suh, K.S. Shin, Structural features of immunostimulatory polysaccharide purified from pectinase hydrolysate of barley leaf, Int. J. Biol. Macromol. 87 (2016) 308–316.
[42] S.S. Ferreira, C.P. Passos, P. Madureira, M. Vilanova, M.A. Coimbra, Structure-function relationships of immunostimulatory polysaccharides: A review, Carbohyd. Polym. 132 (2015) 378–396.
[43] C.S. Nergard, T. Matsumoto, M. Inngjerdingen, K. Inngjerdingen, S. Hokputsa, S. E. Harding, T.E. Michaelsen, D. Diallo, H. Kiyohara, B.S. Paulsen, H. Yamada, Structural and immunological studies of a pectin and a pectic arabinogalactan from *Vernonia kotschyana* Sch, Bip. Ex Walp. (*Asteraceae*), Carbohydr. Res. 340 (2005) 115–130.
[44] N.S. Trede, D.M. Langenau, D. Traver, T. Look, L.I. Zon, The use of zebrafish to understand immunity, Immunity 20 (2004) 367–379.
[45] Y. Li, C. Ran, K. Wei, Y. Xie, M. Xie, W. Zhou, Y. Yang, Z. Zhang, H. Lv, X. Ma, Z. Zhou, The effect of *Astragalus* polysaccharide on growth, gut and liver health, and anti-viral immunity of zebrafish, Aquaculture 540 (2021) 736677.
[46] W. Liu, K. Li, H. Zhang, Y. Li, Z. Lin, J. Xu, Y. Guo, An antitumor arabinan from *Glehnia littoralis* activates immunity and inhibits angiogenesis, Int. J. Biol. Macromol. 263 (2024) 130242.
[47] R. Zhan, L. Xia, J. Shao, C. Wang, D. Chen, Polysaccharide isolated from Chinese jujube fruit (*Zizyphus jujuba* cv. Junzao) exerts anti-inflammatory effects through MAPK signaling, J. Funct. Foods 40 (2018) 461–470.
[48] X. Ao, J. Yan, S. Liu, S. Chen, L. Zou, Y. Yang, L. He, S. Li, A. Liu, K. Zhao, Extraction, isolation and identification of four phenolic compounds from *Pleioblastus amarus* shoots and their antioxidant and anti-inflammatory properties *in vitro*, Food Chem. 374 (2022) 131743.
[49] S. Jiang, H. Yin, X. Qi, W. Song, W. Shi, J. Mou, J. Yang, Immunomodulatory effects of fucosylated chondroitin sulfate from *Stichopus chloronotus* on RAW 264.7 cells, Carbohyd. Polym. 251 (2021) 117088.
[50] W. Ikeda-Ohtsubo, A. Lopez Nadal, E. Zaccaria, M. Iha, H. Kitazawa, M. Kleerebezem, S. Brugman, Intestinal microbiota and immune modulation in zebrafish by fucoidan from Okinawa Mozuku (*Cladosiphon okamuranus*), Front. Nutr. 7 (2020) 67.
[51] J.M. Bates, E. Mittge, J. Kuhlman, K.N. Baden, S.E. Cheesman, K. Guillemin, Distinct signals from the microbiota promote different aspects of zebrafish gut differentiation, Dev. Biol. 297 (2006) 374–386.
[52] G. Roeselers, E.K. Mittge, W.Z. Stephens, D.M. Parichy, C.M. Cavanaugh, K. Guillemin, J.F. Rawls, Evidence for a core gut microbiota in the zebrafish, ISME J. 5 (2011) 1595–1608.
[53] J.Y. Yoo, M. Groer, S.V.O. Dutra, A. Sarkar, D.I. McSkimming, Gut microbiota and immune system interactions, Microorganisms 8 (2020) 1587.
[54] C.J. Solis, M. Poblete-Morales, S. Cabral, J.A. Valdes, A.E. Reyes, R. Avendano-Herrera, C.G. Feijoo, Neutrophil migration in the activation of the innate immune response to different *Flavobacterium psychrophilum* vaccines in zebrafish (*Danio rerio*), J. Immunol. Res. 2015 (2015) 515187.
[55] M.X. Chang, P. Nie, L.L. Wei, Short and long peptidoglycan recognition proteins (PGRPs) in zebrafish, with findings of multiple PGRP homologs in teleost fish, Mol. Immunol. 44 (2007) 3005–3023.
[56] D.S. Weiss, J.R. Sheldon, L.E. Himmel, D.E. Kunkle, A.J. Monteith, K.N. Maloney, E.P. Skaar, Lipocalin-2 is an essential component of the innate immune response to *Acinetobacter baumannii* infection, PLOS Pathog. 18 (2022) e1010809.
[57] M. Kanther, J.F. Rawls, Host–microbe interactions in the developing zebrafish, Curr. Opin. Immunol. 22 (2010) 10–19.
[58] C. Hu, Y. Bai, B. Sun, L. Tang, L. Chen, Significant impairment of intestinal health in zebrafish after subchronic exposure to methylparaben, Sci. Total Environ. 838 (2022) 156389.
[59] C. Bai, F. Su, W. Zhang, H. Kuang, A systematic review on the research progress on polysaccharides from fungal traditional Chinese medicine, Molecules 28 (2023) 6816.
[60] M. Tabbaa, M. Golubic, M.F. Roizen, A.M. Bernstein, Docosahexaenoic acid, inflammation, and bacterial dysbiosis in relation to periodontal disease, inflammatory bowel disease, and the metabolic syndrome, Nutrients 5 (2013) 3299–3310.
[61] S. Gutierrez, S.L. Svahn, M.E. Johansson, Effects of omega-3 fatty acids on immune cells, Int. J. Mol. Sci. 20 (2019) 5028.
[62] V.B. O'Donnell, R.C. Murphy, New families of bioactive oxidized phospholipids generated by immune cells: identification and signaling actions, Blood 120 (2012) 1985–1992.